Plasmonic-enhanced polymer photovoltaic devices incorporating solution-processable metal nanoparticles

Fang-Chung Chen, Jyh-Lih Wu, Chia-Ling Lee, Yi Hong, Chun-Hong Kuo, and Michael H. Huang

---

Articles you may be interested in

Performance improvement of inverted polymer solar cells by doping Au nanoparticles into TiO2 cathode buffer layer
Appl. Phys. Lett. **103**, 233303 (2013); 10.1063/1.4840319

Efficiency enhancement of polymer solar cells by localized surface plasmon of Au nanoparticles
J. Appl. Phys. **114**, 163102 (2013); 10.1063/1.4827181

Plasmonic-enhanced performance for polymer solar cells prepared with inverted structures
Appl. Phys. Lett. **101**, 193902 (2012); 10.1063/1.4766736
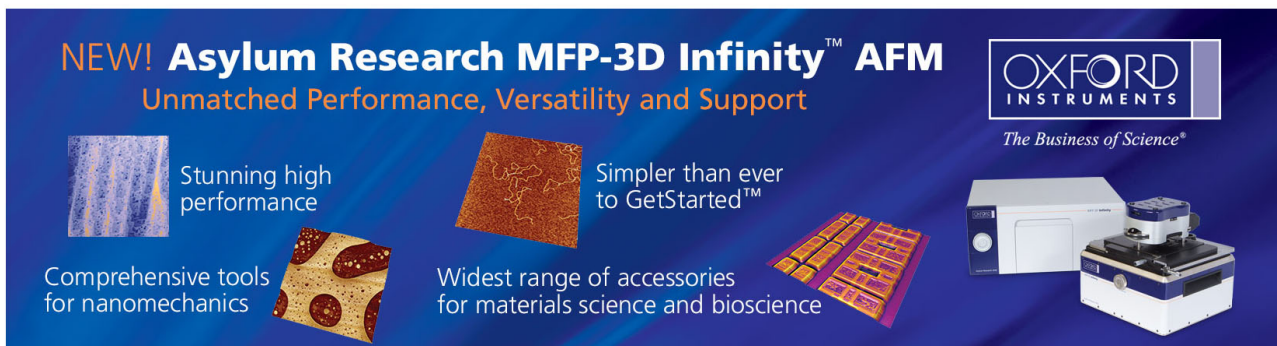
Hybrid polymer:colloidal nanoparticle photovoltaic cells incorporating a solution-processed, multi-functioned ZnO nanocrystal layer
J. Appl. Phys. **111**, 044323 (2012); 10.1063/1.3689154

Efficiency enhancement of polymer photovoltaic devices hybridized with ZnO nanorod arrays by the introduction of a vanadium oxide buffer layer
Appl. Phys. Lett. **93**, 063308 (2008); 10.1063/1.2972113

Plasmonic-enhanced polymer photovoltaic devices incorporating solution-processable metal nanoparticles

Fang-Chung Chen,[1,2,a)] Jyh-Lih Wu,[1,3] Chia-Ling Lee,[1,2] Yi Hong,[1,2] Chun-Hong Kuo,[4] and Michael H. Huang[4]

[1]*Department of Photonics, National Chiao Tung University, Hsinchu 30010, Taiwan*
[2]*Display Institute, National Chiao Tung University, Hsinchu 30010, Taiwan*
[3]*Institute of Electro-optical Engineering, National Chiao Tung University, Hsinchu 30013, Taiwan*
[4]*Department of Chemistry, National Tsing Hua University, Hsinchu 30013, Taiwan*

We have explored the effect of gold nanoparticle (Au NP)-induced surface plasmons on the performance of organic photovoltaic devices (OPVs). The power conversion efficiency of these OPVs was improved after blending the Au NPs into the anodic buffer layer. The addition of Au NPs increased the rate of exciton generation and the probability of exciton dissociation, thereby enhancing the short-circuit current density and the fill factor. We attribute the improvement in device performance to the local enhancement in the electromagnetic field originating from the excitation of the localized surface plasmon resonance. © *2009 American Institute of Physics.*
[DOI: 10.1063/1.3174914]

Organic photovoltaic (OPV) devices are promising green energy systems that possess many advantageous properties, such as light weight, low cost, fabrication at low temperature, and mechanical flexibility.[1,2] The introduction of a donor/acceptor bulk heterojunction provides a large phase-separated interfacial area for efficient exciton dissociation, which dramatically improves the power conversion efficiency (PCE).[3,4] The most efficient model donor/acceptor system to date comprises of poly(3-hexylthiophene) (P3HT) and [6,6]-phenyl-C_{61}-butyric acid methyl ester (PCBM). The corresponding OPV devices exhibit efficiencies of up to 5%.[5–7] One of the key issues toward achieving high performance is sufficient photon absorption of the photoactive layer, i.e., efficient harvesting of sunlight. Nevertheless, the use of a thicker active layer inevitably leads to increased device resistance because of the low carrier mobilities of organic materials.[8,9] An alternative approach toward enhanced light absorption without the need for thick films is the exploitation of localized surface plasmon resonance (LSPR).[10–12] The excitation of LSPR through the resonant interaction between the electromagnetic field of incident light and the surface electron density surrounding metallic nanoparticles (NPs) causes local enhancement in the electromagnetic field, which is expected to enhance light harvesting in the OPV devices.[13–16] In this study, we developed a simple method—doping Au NPs into the poly(3,4-ethylenedioxythiophene):poly(styrene sulfonate) (PEDOT:PSS) buffer layer—to improve the device performance of OPVs. We also investigated the effect of the Au NP-induced LSPR on the photocurrent. Compared with existing approaches toward plasmonic-enhanced OPVs, the method we report herein is simpler and the size and density of the NPs is easier to control.

To prepare the composite buffer layer, a Au NP solution was blended into the PEDOT:PSS solution at various concentrations. The volume ratios of the Au NP solution were

10%, 20%, and 30%. The Au NP solution was prepared using a procedure based on our previous report.[17] The particles have a somewhat spherical appearance. The average particle size of the Au NPs estimated from scanning electron microscopy (SEM) images was approximately 30–40 nm. The size of the NPs was intentionally selected in order to let the resonance peak match the absorption of the photoactive layer of the device. The inset of Fig. 1(a) presents a schematic repre-
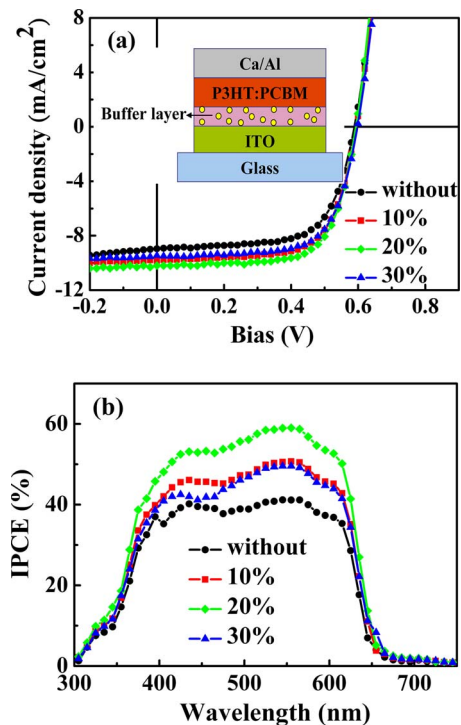
FIG. 1. (Color online) (a) *J-V* characteristics, recorded under AM 1.5G illumination at 100 mW cm^{-2}, of devices incorporating PEDOT:PSS doped with various concentrations of Au NP solutions: without doping (○); 10% Au NP solution doping (■); 20% Au NP solution doping (◆); and 30% Au NP solution doping (▲). (b) Corresponding IPCE curves of these OPV devices. Inset: schematic representation of the device structure of the photovoltaic devices.

a)Author to whom correspondence should be addressed. Electronic mail: fcchen@mail.nctu.edu.tw.

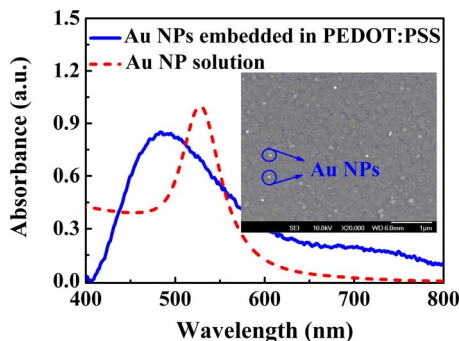FIG. 2. (Color online) Absorption spectra of Au NPs embedded in the PEDOT:PSS matrix (solid line) and in solution (dashed line). Inset: SEM image of the PEDOT:PSS film prepared with 20% Au NP solution blended into the matrix. A neat PEDOT:PSS film was used as the baseline for measurement of the absorption of the PEDOT:PSS composite films.

sentation of the device structure. To fabricate the OPV device, the buffer layer was spin-coated onto an indium tin oxide-coated glass substrate and then the system was subjected to thermal annealing at 120 °C for 1 h. The inset of Fig. 2 displays a SEM image of the resulting film with its embedded Au NPs. A solution of P3HT/PCBM (1:1, w/w) in 1,2-dichlorobenzene was spin-coated on top of the buffer layer. After performing a solvent annealing process,[2] the polymer film was thermally annealed at 110 °C for 15 min in a glove box. Finally, the metals Ca (30 nm) and Al (100 nm) were deposited sequentially through thermal evaporation to form the bilayer cathode. The device area, defined through a shadow mask, was 0.12 cm^2. The current density-voltage (J-V) characteristics of the OPVs were measured using a Keithley 2400 source measure unit. The photocurrent response was obtained under illumination from a 150 W thermal Oriel solar simulator (AM 1.5G). The illumination intensity was calibrated using a standard Si photodiode equipped with a KG-5 filter (Hamamatsu, Inc.).[18] The absorption spectra of Au NPs were measured using a Perkin–Elmer Lambda 950 ultraviolet/visible/near infrared spectrometer.

Figure 1(a) displays the J-V characteristics, recorded under 100 mW cm^{-2} illumination (AM 1.5G), of the OPV devices prepared with buffer layers incorporating various amounts of Au NPs. The reference device prepared with pristine PEDOT:PSS exhibited an open-circuit voltage (V_{oc}) of 0.59 V, a short-circuit current (J_{sc}) of 8.95 mA cm^{-2}, and a fill factor (FF) of 65.9%. The calculated PCE was 3.48%. After the addition of Au NPs to the buffer layer, the values of V_{oc} remained unchanged (0.59 V) but the FFs improved considerably (Table I). We also observed a noticeably upward trend in the values of J_{sc} after introducing the Au NPs. For

the devices prepared with PEDOT:PSS blended with 10% and 20% Au NP solutions, these values were 9.50 and 10.18 mA cm^{-2}, respectively, with the PCEs increasing to 3.89% and 4.19%, respectively. On the other hand, a further increase in the concentration of the Au NP solution to 30% led to a decrease in the value of J_{sc}, presumably due to enhanced backward scattering and/or increased resistivity of the buffer layer. From the result of the four-point probe measurement, we found that the resistivity of the buffer layers increased after embedding the Au NPs (Table I). We suspect that this behavior arose from a possible change in the morphology of the PEDOT:PSS blend. Accordingly, the values of the device series resistance (R_s) extracted from the inverse slopes of the dark J-V curves at a voltage of 1.5 V also increased after incorporating the Au NPs (Table I), revealing that the enhanced performance of the OPV devices did not result from a reduction in device resistance. Table I summarizes the device characteristics.

Figure 1(b) displays the incident photon-to-electron conversion efficiency (IPCE) curves of our various devices. The trends in the IPCE follow those for the values of J_{sc}. Within the wavelength range from 400 to 600 nm, the photocurrent increased notably after incorporating the Au NPs. The wavelength range of spectral response enhancement coincides with the excitation range of Au NPs (Fig. 2), indicating that excitation of the LSPR indeed improved the photocurrent. Note that the absorption peak of the Au NP solution was located at approximately 530 nm, whereas that of the Au NPs embedded in the PEDOT:PSS blend was located at approximately 490 nm (Fig. 2). This phenomenon is associated with the resonance peak of NPs depending strongly on their surrounding media.[13,14,16]

To further investigate the underlying mechanism responsible for the enhanced performance of the devices, we compared the maximum exciton generation rates (G_{max}) and exciton dissociation probabilities for devices prepared using pristine PEDOT:PSS and PEDOT:PSS doped with 20% Au NP solution, following the analytical approach reported by Mihailetchi and co-workers.[19,20] Figure 3 reveals the effect of the LSPR on the photocurrent density (J_{ph}). We determined the value of J_{ph} using the equation $J_{ph} = J_L - J_D$, where J_L and J_D are the current densities under illumination and in the dark, respectively. The plot of J_{ph} with respect to the effective voltage ($V_{eff} = V_o - V_a$), where V_o is the voltage when J_{ph} equals zero (i.e., $J_L = J_D$) and V_a is the applied voltage, reveals two distinct regimes; one where the value of J_{ph} increased linearly with increasing voltage at a low value of V_{eff} and another where it reached a saturated level at a sufficiently high value of V_{eff}. The saturation photocurrent

TABLE I. Photovoltaic characteristics of OPVs incorporating PEDOT:PSS doped with various concentrations of Au NP solutions.

	V_{oc} (V)	J_{sc} (mA cm^{-2})	FF (%)	R_s [a] (Ω cm^2)	Resistivity[b] (Ω cm)	PCE (%)
Pristine PEDOT:PSS	0.59	8.95	65.9	1.73	32.0	3.48
10% Au NP solution	0.59	9.50	69.2	1.86	37.1	3.89
20% Au NP solution	0.59	10.18	69.8	2.08	43.5	4.19
30% Au NP solution	0.59	9.46	69.3	2.35	47.5	3.87

[a]Device series resistance (R_s) of the OPV obtained from the inverse slope of the dark J-V curve at a voltage of 1.5 V.
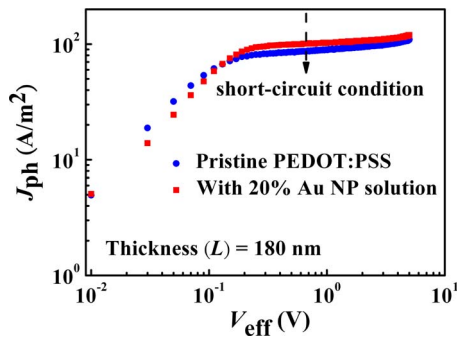[b]Resistivity of the buffer layer determined using the four-point probe method.

FIG. 3. (Color online) Plots of photocurrent density (J_{ph}) with respect to the effective bias (V_{eff}) for devices incorporating pristine PEDOT:PSS and PEDOT:PSS containing 20% Au NP solution.

density (J_{sat}), which is independent of the bias and temperature, correlates with the value of G_{max}, given by $J_{sat} = qG_{max}L$, where q is the electronic charge and L is the thickness of the active layer ($L = 180$ nm). As a result, the values of J_{sat} for the devices prepared with pristine PEDOT:PSS and PEDOT:PSS doped with 20% Au NP solution were 110 and 119 A m^{-2}, respectively, and the calculated values of G_{max} were 3.82×10^{27} and 4.13×10^{27} m^{-3} s^{-1}, respectively. Because the value of G_{max} is governed only by the absorption of light,[19,20] the enhanced value suggests that the incorporation of the Au NPs increased the degree of light harvesting in the devices.

The exciton dissociation probability can be obtained from the normalized photocurrent density (J_{ph}/J_{sat}).[19,21] After incorporating 20% Au NP solution in the PEDOT:PSS blend, the exciton dissociation probability under the short-circuit condition ($V_a = 0$ V) increased from 78.7% to 84.9%, indicating that excitation of the LSPR facilitated the excitons to dissociate into free carriers. In general, an increase in the exciton dissociation probability reduces the recombination rate and, therefore, improves the FFs of OPVs.[22,23] Consequently, we primarily attribute the increased FF observed in Fig. 1 to the increased exciton dissociation probability resulting from the local enhancement in the electromagnetic field originating from excitation of the LSPR.

In summary, we have improved the device performance of OPVs after blending Au NPs into the PEDOT:PSS layer. The unique optical properties of the LSPR, induced by the Au NPs, led to a noticeable enhancement in the photocurrent. From the observed increase in the FF, we deduced that excitation of the LSPR increased not only the rate of exciton generation but also the probability of exciton dissociation. Finally, we note that this approach is quite simple and may be suitable for application to the low-temperature processes used to form flexible OPVs on plastic substrates.

[1] C. J. Brabec, N. S. Sariciftci, and J. C. Hummelen, Adv. Funct. Mater. **11**, 15 (2001).
[2] G. Li, V. Shrotriya, J. S. Huang, Y. Yao, T. Moriarty, K. Emery, and Y. Yang, Nature Mater. **4**, 864 (2005).
[3] N. S. Sariciftci, L. Smilowitz, A. J. Heeger, and F. Wudl, Science **258**, 1474 (1992).
[4] G. Yu, J. Gao, J. C. Hummelen, F. Wudl, and A. J. Heeger, Science **270**, 1789 (1995).
[5] C. J. Ko, Y. K. Lin, F. C. Chen, and C. W. Chu, Appl. Phys. Lett. **90**, 063509 (2007).
[6] W. L. Ma, C. Y. Yang, X. Gong, K. Lee, and A. J. Heeger, Adv. Funct. Mater. **15**, 1617 (2005).
[7] M. Reyes-Reyes, K. Kim, and D. L. Carroll, Appl. Phys. Lett. **87**, 083506 (2005).
[8] V. Shrotriya, E. H. E. Wu, G. Li, Y. Yao, and Y. Yang, Appl. Phys. Lett. **88**, 064104 (2006).
[9] A. Yakimov and S. R. Forrest, Appl. Phys. Lett. **80**, 1667 (2002).
[10] S. S. Kim, S. I. Na, J. Jo, D. Y. Kim, and Y. C. Nah, Appl. Phys. Lett. **93**, 073307 (2008).
[11] J. H. Lee, J. H. Park, J. S. Kim, D. Y. Lee, and K. Cho, Org. Electron. **10**, 416 (2009).
[12] A. J. Morfa, K. L. Rowlen, T. H. Reilly, M. J. Romero, and J. van de Lagemaat, Appl. Phys. Lett. **92**, 013504 (2008).
[13] E. Hutter and J. H. Fendler, Adv. Mater. (Weinheim, Ger.) **16**, 1685 (2004).
[14] K. L. Kelly, E. Coronado, L. L. Zhao, and G. C. Schatz, J. Phys. Chem. B **107**, 668 (2003).
[15] S. Lal, S. Link, and N. J. Halas, Nat. Photonics **1**, 641 (2007).
[16] M. Pelton, J. Aizpurua, and G. Bryant, Laser Photonics Rev. **2**, 136 (2008).
[17] C. C. Chang, H. L. Wu, C. H. Kuo, and M. H. Huang, Chem. Mater. **20**, 7570 (2008).
[18] V. Shrotriya, G. Li, Y. Yao, T. Moriarty, K. Emery, and Y. Yang, Adv. Funct. Mater. **16**, 2016 (2006).
[19] V. D. Mihailetchi, L. J. A. Koster, J. C. Hummelen, and P. W. M. Blom, Phys. Rev. Lett. **93**, 216601 (2004).
[20] V. D. Mihailetchi, H. X. Xie, B. de Boer, L. J. A. Koster, and P. W. M. Blom, Adv. Funct. Mater. **16**, 699 (2006).
[21] V. Shrotriya, Y. Yao, G. Li, and Y. Yang, Appl. Phys. Lett. **89**, 063505 (2006).
[22] L. J. A. Koster, V. D. Mihailetchi, and P. W. M. Blom, Appl. Phys. Lett. **88**, 052104 (2006).
[23] M. M. Mandoc, W. Veurman, L. J. A. Koster, B. de Boer, and P. W. M. Blom, Adv. Funct. Mater. **17**, 2167 (2007).